J. Biochem. **139**, 383–390 (2006)
doi:10.1093/jb/mvj046

Characterization and Application of a Novel RNA Aptamer against the Mouse Prion Protein

Satoru Sekiya[1,2], Ken Noda[3], Fumiko Nishikawa[4], Takashi Yokoyama[5], Penmetcha K.R. Kumar[4] and Satoshi Nishikawa[1,2,*]

[1]Cooperative Graduate School, University of Tsukuba, Tennodai, Tsukuba, Ibaraki; [2]Age Dimension Research Center, National Institute of Advanced Industrial Science and Technology (AIST), Tsukuba, Ibaraki; [3]National Veterinary Assay Laboratory, Ministry of Agriculture, Forestry & Fisheries, Kokubunji, Tokyo; [4]Institute for Biological Resources and Functions, AIST, Tsukuba, Ibaraki; and [5]Prion Disease Research Center, National Institute of Animal Health (NIAH), Tsukuba, Ibaraki

Received October 18, 2005; accepted December 13, 2005

In order to isolate RNA aptamers against the mouse prion protein (mPrP), we carried out *in vitro* selection from RNA pools containing a 30-nucleotide randomized region. Aptamer 60-3 was found to have a high affinity for mPrP (K_d = 5.6 ± 1.5 nM), and 2′-fluoro-pyrimidine modifications for RNase resistance did not abolish its binding activity (K_d = 22 ± 4 nM). Following 5′ biotinylation, aptamer 60-3 specifically detected PrP in mouse brain homogenate in a Northwestern blotting assay. To determine the mPrP–aptamer binding region, we performed protein-deletion-mutant analysis and competition-binding analysis using heparin. The results showed that aptamer 60-3 appears to have binding sites located between amino acids 23–108.

Key words: blotting assay, *in vitro* selection, prion, RNA aptamer.

Prions are infectious particles that are devoid of nucleic acids and are composed exclusively of misfolded proteins. The prion protein (PrP) (*1*) has two alternative forms: a normal cellular protein (PrP^C), which is a soluble α-helix–rich cellular isoform; and an insoluble β-sheet–rich abnormal isoform known as the protease-resistant form (PrP^{Sc}). The conformational change from PrP^C to PrP^{Sc} is thought to be crucial in prion pathogenesis (*2, 3*), causing diseases such as Creutzfeldt–Jacob disease (CJD) and Gerstmann–Straussler–Scheinker syndrome in humans, bovine spongiform encephalopathy (BSE) in cattle, chronic wasting disease in elk and scrapie in sheep and goats. Several lines of evidence suggest that minute amounts of PrP^{Sc} elicit clinical symptoms, enabling host PrP^C to convert into large amounts of the PrP^{Sc} form (*4*, *5*). Recently, an efficient *in vitro* conversion was achieved using 1×10^4 molecules of PrP^{Sc} (*6*, *7*). Interestingly, the *in vitro* PrP^{Sc} form shared similar biochemical and structural properties with PrP^{Sc} from diseased animal brains. However, the detailed mechanism that mediates the conversion of PrP^C to the PrP^{Sc} form remains unknown.

Transmission of prion diseases between cattle and humans is well documented, with PrP^{Sc}-infected beef validated as a cause of variant CJD in humans (*8*). In order to avoid future prion-disease transmission, it is imperative to detect PrP^{Sc}. The current detection method for PrP^{Sc} uses an ELISA based test, Western blotting analysis and immunohistochemical analysis using antibodies that might not clearly distinguish between PrP^C and PrP^{Sc}. A proteinase-digestion step has consequently been introduced (*9–11*) to digest host PrP^C completely and leave the protease-resistant PrP^{Sc} fragment in the homogenate. Although the current methodology enables the detection of minute amounts of PrP^{Sc}, it fails to identify the intermediate form or relative mild forms of PrP^{Sc} that are digested during protease incubation, thus weakening the test sensitivity.

Yokoyama *et al*. previously reported a histoblot analysis of scrapie infected mouse brains showing that a decrease in PrP^C correlates with an accumulation of PrP^{Sc} (*12*). However, no decrease in mRNA-expression levels of the PrP gene (*Prnp*) could be detected, suggesting that depletion of the PrP^C protein is primarily responsible for increasing levels of PrP^{Sc}. The study also provides a molecular basis for the notion that a decrease of soluble PrP^C in the brain homogenate is directly correlated with the onset of pathogenesis of the central nervous system. However, a decrease in PrP^C has not been reported in any other central nervous system disease, indicating the importance of the specific monitoring of brain homogenate PrP^C levels.

We employed *in vitro*-selection technology (*13*, *14*) using random RNA pools to find a suitable molecule that binds specifically to PrP^C. We focused on aptamers, which are nucleic-acid ligands that recognize a wide range of target molecules with high affinity and specificity (reviewed in Ref. *15*). Their binding affinities are comparable to, or higher than, those of antibodies and antigens. Moreover, aptamer binding uses only a small region of the target molecule, in comparison with antibodies. They are also able to distinguish between closely related molecules; for example, the anti-theophyllin aptamer binds specifically to theophyllin with a binding affinity over 14,000-fold greater than that for caffeine, even though the two molecules differ only in the presence or absence of a methyl group at the N7 position (*16*).

In the current study, we isolated an RNA aptamer with a high affinity for mouse PrP (mPrP; amino acids 23–230).

*To whom correspondence should be addressed at: Age Dimension Research Center, National Institute of Advanced Industrial Science and Technology (AIST), Higashi, Tsukuba, Ibaraki 305–8566. Tel: +81-29-861-6097, Fax: +81-29-861-6095, E-mail: satoshi-nishikawa@aist.go.jp

The 2′-fluoro (F)–modified aptamer that is stabilized against ribonuclease digestion also binds to mPrP. We developed a sensitive Northwestern blotting assay using the 2′-F-modified aptamer to analyze PrP^{C} levels in mouse brain homogenate.

MATERIALS AND METHODS

PrP Preparation—Recombinant mPrP (amino acids 23–230) and bPrP (amino acids 25–241) were purchased from Prionics (Switzerland). Truncated mPrP ($mPrP^{120–230}$; amino acids 120–230) was purchased from Alicon AG (Switzerland). A mPrP–GST fusion protein [with GST fused to the amino (N)-terminus] and deletion mutants GST–$mPrP^{23–230}$, GST–$mPrP^{89–230}$ and GST–$mPrP^{155–230}$ were prepared using expression plasmids [from Dr. Imamura, Prion Disease Research Center, National Institute of Animal Health (NIAH)] using a GST fusion protein-expression system according to the manufacturer's instructions (Amersham Biosciences). Protein concentration was measured using a Bio-Rad protein assay kit (Hercules).

In Vitro *Selection of RNA Aptamer*—An N30H RNA pool [5′-GGUAGAUACGAUGGA-(N30)-CAUGACGCGCA-GCCA-3′] described previously (*17*) was used to perform *in vitro* selection on a 0.45-μm HAWP nitrocellulose filter (Millipore). RNAs were heat denatured at 95°C for 2 min and cooled to room temperature for 2 h in reaction buffer [20 mM Tris-HCl (pH 7) and 100 mM NaCl] prior to use. The detailed selection conditions are described in Table 1. For the first round of selection, the RNA pool was incubated for 60 min with mPrP in the reaction buffer at room temperature. This mixture was passed through the nitrocellulose filter and washed twice with 500 μl reaction buffer. RNA bound to mPrP on the filter was recovered with 500 μl elution buffer [7 M urea, 0.4 M sodium acetate (pH 5.5) and 5 mM EDTA] and extracted by shaking for 2 h at room temperature. The eluted RNA was recovered by ethanol precipitation and reverse transcribed using AMV reverse transcriptase (Roche Applied Science) at 42°C for 1 h. The product was PCR amplified (94°C for 1 min, 50°C for 1 min and 72°C for 1 min) using Gene Taq (Nippon Gene) with proper primers (Espec Oligo Service) (*17*) before being transcribed using the T7 Ampliscribe Kit (Epicentre Technologies) and subjected to the next round of selection. From the sixth round of selection onwards, tRNA (Roche Applied Science) was used as non-specific competitor and anti-mPrP aptamers obtained from a different RNA library (N30V, data not shown) were used as a specific competitors in the reaction mixture. At the ninth round of selection, magnetic beads (Dynabeads M-450 Epoxy; Dynal Biotech) were used instead of the nitrocellulose membrane for protein fixation. The cDNA pool obtained after the tenth round of selection was inserted into the pGEM-Easy-T vector (Promega), cloned in *Escherichia coli* JM109 strain and sequenced (ABI Prism 377 DNA sequencer; Applied Biosystems). The secondary structure models of selected aptamers were drawn with the MUL-Fold program based on the Zuker algorithm (*18*).

Table 1. ***In vitro* selection conditions for the isolation of an anti-mPrP aptamer.**

Round of selection	RNA (μM)	mPrP (μM)	tRNA (μM)	N30V-G10RNA pool (μM)	Time (min)
1	6	1.2	0	0	60
2	2	0.6	0	0	60
3	1.6	0.3	0	0	60
4	2	0.05	0	0	60
5	2	0.05	0	0	30
6	2	0.05	100	10	10
7	2	0.05	200	20	10
8	2	0.05	500	50	10
9	2	0.54 (M-450)	20	0	10
10	2	0.05	800	80	5

Preparation of RNA—To prepare RNA aptamer, the double-stranded DNA generated by PCR was used as a template for *in vitro* transcription by T7 RNA polymerase as described above. The 2′-F pyrimidine RNA aptamer 60-3F was prepared using a Durascribe transcription kit (Epicetre). The chemically synthesized 5′-biotinylated 2′-OMe pyrimidine RNA aptamer 60-3OMe was purchased from Greiner (Germany).

Binding Assay of Anti-mPrP Aptamer—Radioisotope labeling of RNA by *in vitro* transcription was carried out as previously described (*19*). Labeled 2′-fluoro (F) RNA was prepared by *in vitro* transcription (Durascribe™, Epicentre) with α-^{32}P-ATP. Refolded labeled aptamer (10 nM) was mixed with 0–2 μM mPrP or its derivatives in the presence of 100 nM $(U)_{16}$ oligonucleotide as a non-specific competitor in a total volume of 25 μl. After 10 min incubation, the mixture was passed through a nitrocellulose filter and washed twice with 250 μl reaction buffer. The amount of bound RNA was measured with a BAS 2500 (Fuji Film), and binding activities were calculated as the percentage of input RNA retained on the filter in the protein/RNA complex. We determined the equilibrium dissociation constant (K_d) by GraphPad PRISM using a non-linear regression-curve fitting and one site binding hyperbola equation: RNA binding = $B_{max} \times [PrP]/(K_d + [PrP])$.

Enzymatic Probing of Aptamer 60-3—5′-[^{32}P]–labeled aptamer 60-3 was partially digested with RNase T1 (Roche Applied Science) and RNase A (Wako) as previously described (*19*). Labeled RNA was mixed with 0.1 U RNase T1 or 10 ng RNase A with 5 μg total tRNA in reaction buffer [20 mM Tris-HCl (pH 7.5) and 100 mM NaCl], incubated at room temperature for 1 min and stopped by adding loading buffer (*19*). For an alkaline ladder, labeled aptamer 60-3 was hydrolyzed in 10 μl alkaline solution (50 mM sodium carbonate, pH 9.2) by heating at 90°C for 5 min with 5 μg carrier tRNA. Digested products were separated by 8% PAGE containing 7 M urea and analyzed with BAS2500 (Fuji Film).

Competitive-Binding Assay with Heparin Using BIACORE—The aptamer–protein binding affinity in the presence of heparin was determined using SPR technology. Aptamer 60-3 with a 15 nucleotide (nt) oligo (A) tail at the 3′ end (pA60-3) was synthesized by *in vitro* transcription of a mutagenic PCR product. A competitive-binding assay was performed using the BIACORE 2000 instrument with HBS-P [10 mM HEPES (pH 7.5), 150 mM NaCl and 0.05% Tween-20] running buffer and sample dilution buffer in the following steps (*20*). First, 0.5 μM 5′ biotinylated $(dT)_{24}$ (Bi-dT, 5 μl) was bound to the surface of a streptavidin-coated sensor chip (SA chip; Biacore) at a

flow rate of 2 μl/min [approximately 1,200 resonance units (RU) immobilized]. Second, 50 nM pA60-3 was immobilized by hybridization at a flow rate of 2 μl/min for 10 min (approximately 1,600–1,700 RU). Third, the analyte was injected at a flow rate of 20 μl/min for 2 min (association), followed by running buffer for 2 min (dissociation). For the regeneration stage, the bound analyte and pA60-3 were washed with 5 μl 50 mM NaOH at a flow rate of 60 μl/min. The second and third steps were repeated for each analyte. To correct the background response values, the sensorgram of buffer alone was subtracted from the signal recorded at the same surface.

The effect of heparin (porcine heparin; ICN biochemicals) on RNA–mPrP variant binding was investigated using a range of heparin concentrations (0, 0.1, 0.4 and 2 ng/μl) and 10 nM mPrP or 100 nM GST-mPrP$^{89–230}$. The observed binding differences after injection of analyte (ΔRU) were plotted against the range of heparin concentrations.

Precipitation of PrPs by 60-3F Aptamer—The pyrimidine 2′-F RNA aptamer was transcribed using a Durascribe™ transcription kit, and 5′-end biotin labeling (Vector Lab.) was carried out according to the manufacturer's instructions. A suspension (10 μl) streptavidin coated magnetic beads (Magnabind, Pierce) was incubated with 10 μl of 20 nM 5′-biotinylated 2′-F aptamer (60-3Fb) and blocked with 2% BSA, then mixed with 500 μl of 0.25% mouse brain homogenate and incubated for 30 min at room temperature. The magnet-precipitation was washed and suspended in 40 μl of SDS-PAGE sample buffer (Prionics). Ten-microlitter aliquots were run on a Novex 12% gel (Invitrogen), transferred to a PVDF membrane and stained with monoclonal antibody 6H4 (Prionics).

Northwestern Blotting Assay with Aptamer 60-3F—The Northwestern assay was performed using conventional methods (*21*). A sample of 10 μl 10% ddY mouse brain homogenate in suspension buffer [0.1% Nonidet P-40, 0.1% deoxycholate, 20 mM Tris-HCl (pH 7.5) and 100 mM NaCl] was separated by 10% SDS-PAGE and transferred to a 0.22 μm nitrocellulose membrane (Bio-Rad) at 4°C for 1 h. A sample of 5 ml 1% BSA in selection buffer was used for a 1-h primary blocking step, followed by 1-h secondary blocking using 5 ml of poly (U) (0.5 mg/ml) (Amersham Bioscience) in selection buffer. A 1-h incubation with 200 nM 60-3Fb, poly (U) (0.5 mg/ml) and 0.1% BSA was followed by a 1-h incubation with streptavidin–alkaline phosphatase conjugate (2 ng/μl) (SA–AP; Roche Applied Science) in selection buffer and a 30-s incubation with CDP-Star (20 mg/ml) (Roche Applied Science). Detection was carried out with an ECL Mini-Camera (Amersham Bioscience) and Polaroid film. All incubations were performed at room temperature. For standard immunoblotting assay of PrP^{C}, we used 6H4 antibody (Prionics). In the case of radioisotope labeling, the aptamer was labeled as described above.

Dot-Blotting Assay—Recombinant mPrP (15.5–250 ng) was spotted onto a 0.45-μm nitrocellulose membrane (Bio-Rad) and air-dried. The membrane was treated by blocking with 2 ml 1% BSA in reaction buffer for 1 h, incubating for 1 h with 200 nM 60–3Fb, and then incubating with SA-AP (2 ng/μl) (Roche Applied Science) in reaction buffer for 1 h. Following a 30-s incubation with CDP-Star (20 mg/ml), detection was carried out with an ECL Mini-Camera and Polaroid film. All procedures were performed at room temperature.

RESULTS

In Vitro *Selection*—We used the recombinant mPrP (amino acids 23–230, Fig. 1) for *in vitro* selection, which generated an RNA library of approximately 10^{14} different molecules (300 pmol) with 30 nt randomized sequences of 60-nt RNA. We applied the following selection pressures: first, decreases in protein concentration and reaction time; second, an increase of tRNA concentration as a non-specific competitor; and third, an increase in the concentration of another anti-mPrP aptamer pool (data not shown) as a specific competitor (Table 1). Furthermore, we used magnetic-bead selection instead of filter selection in the ninth round to exclude system-dependent candidates. The specific-binding ratio (presence/absence of tRNA) of each RNA pool increased with successive selection rounds (data not shown). The maximum specific binding to mPrP occurred at the tenth round of selection, after which 17 clones were sequenced. These were shown to share similar sequences and were classified into three types according to their point mutations (Fig. 2).

Binding Affinity of Aptamer 60-3 for PrPs—We focused on 60-3 as a main clone with the highest affinity for mPrP among the three types of RNA aptamers and determined its K_d by GraphPad PRISM. Binding reactions were carried out using 10 nM aptamer 60-3 and various concentrations of mPrP (ranging from 0.5 to 1,000 nM). Approximately 60–70% maximal binding activity was observed at 100 nM mPrP, and aptamer 60-3 was shown to have a K_d value of 5.6 ± 1.5 nM (Fig. 3).

The binding affinity of aptamer 60-3 for bPrP was found to be K_d = 72 ± 10 nM (Fig. 3), which is a more than 10-fold decrease compared with that of mPrP. As shown in Fig. 1, the main difference between the amino acid sequences of mPrP and bPrP is the number of octapeptide repeat sequences (PHGGGWGQ): mPrP possesses five repeats between amino acids 51 and 91, whereas bPrP possesses six repeats between amino acids 52 and 103.

Nuclease resistance is an important factor in the application of aptamers (*22*, *23*). Therefore, we prepared 2′-F substituted pyrimidine aptamer 60-3 (60-3F) and measured its K_d value against mPrP. Maximal binding to mPrP was found to be higher compared with 60-3, and the K_d value also showed a slight increase (K_d = 22 ± 4 nM; Fig. 3). Furthermore, biotinylation of the 5′ end of aptamer 60-3F did not affect its binding affinity for mPrP; thus, we were able to use it in the Northwestern blotting assay without the radioisotope labeling described later.

Identification of the Aptamer 60-3-mPrP–Binding Region—mPrP–GST fusion proteins of the full-length mPrP sequence (GST–mPrP$^{23–230}$) and deletion mutants GST–mPrP$^{89–230}$ and GST–mPrP$^{155–230}$ were purified from *E. coli* in over 95% homogeneity, and used for the analysis of aptamer binding. GST–mPrP$^{23–230}$ showed a similar binding affinity for 60-3F (K_d = 30 ± 9 nM; Fig. 4) to that of mPrP, suggesting that the fusion of GST does not interfere with binding. By contrast, the K_d value of the deletion variant GST–PrP$^{89–230}$ (433 ± 147 nM; Fig. 4) increased more than 10-fold compared with

```
Mouse:  MANLGYWLLAL--FVTMWTDVGLCKKRPKPGG-WNTGGSRYPGQGSPGGNRYPPQGG-TWGQPHGGGWGQPHGGSWGQPH
Human:  .....C.M.V.---.AT.S.L..........-..........................GG..............G.....
Bovine: .VKSHIGSWI.VL..A..S............G.........................GG..............G.....

Mouse:  GGSWGQPHGGG-WGQ--------GGGTHNQWNKPSKPKTNLKHVAGAAAAGAVVGGLGGYMLGSAMSRPMIHFGNDWEDRYY
Human:  ..G..........-...---------.....S..........M..M.......................I....S.Y.....
Bovine: ..G..........-...PHGGGGWGQGG..G..........M..V.......................L....S.Y.....

Mouse:  RENMYRYPNQVYYRPVDQYSNQNNFVHDCVNITIKQHTVTTTTKGENFTETDVKMMERVVEQMCVTQYQKESQAYYDGRRS
Human:  ....H..........M.E.............................................I...ER.......-Q.G-
Bovine: ....H.............................E..............I...K.......I....R.......-Q.G-

Mouse:  SSTVLFSSPPVILLISFLIFLIVG
Human:  ..M.....................
Bovine: .-VI.....................
```

Fig. 1. **Amino-acid sequence alignment of mPrP, bPrP and human PrP.** The numbering is based on the amino-acid sequence of mPrP. Underlines and double underlines represent the signal peptide and glycosyl-phosphatidyl-inositol (GPI) anchor, respectively. The octapeptide (PHGGGWGQ) repeat region is shown in bold letters. The complete sequence of mPrP is given, but, for the other species, only amino-acid residues that differ with respect to mPrP are indicated.

Type I(8/17 clones)

60-3: *GGUAGAUACGAU*GGAGGUGUAUUUUAUGUGCGUAUUU-GGAGG*CAUGACGCGCAGCCA*

TYPE II(6/17 clones)

60-2: *GGUAGAUACGAU*-GGAGGUGUAUUGCAUGCGUGUGUUU-GGAGG*CAUGACGCGCAGCCA*

Type III(3/17 clones)

60-1: *GGUAGAUACGAU*GGAGGUGUAUUGCAUGCGUGUGUUUUGGAGG*CAUGACGCGCAGCCA*

Fig. 2. **Nucleotide sequences of anti-mPrP aptamers.** 5′- and 3′-primer regions used in PCR are italicized. Aptamer nucleotide sequence variations are underlined.

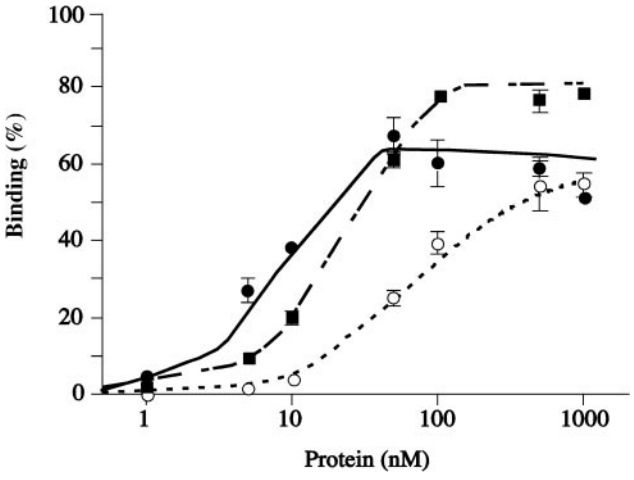

Fig. 3. **Binding affinity of anti-mPrP aptamers for PrPs.** Aptamer 60-3 binding with mPrP is shown by closed circles, aptamer 60-3 binding with bPrP is shown by open circles and 2′-F pyrimidine modified aptamer (60-3F) binding with mPrP is shown by closed squares.

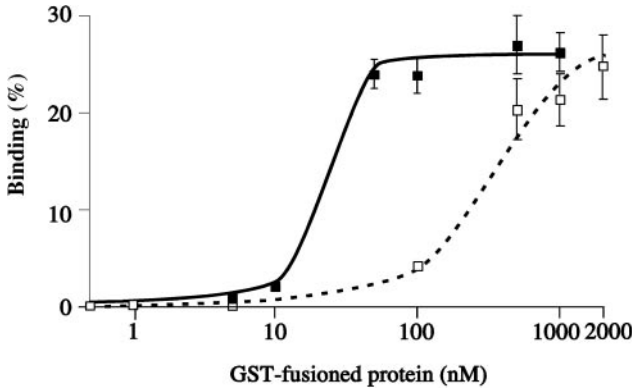

Fig. 4. **Binding affinity of anti-mPrP aptamer for deletion variants of mPrP.** Closed squares represent aptamer 60-3F binding with GST-mPrP$^{23–230}$. Open squares represent 60-3F binding with GST-mPrP$^{89–230}$.

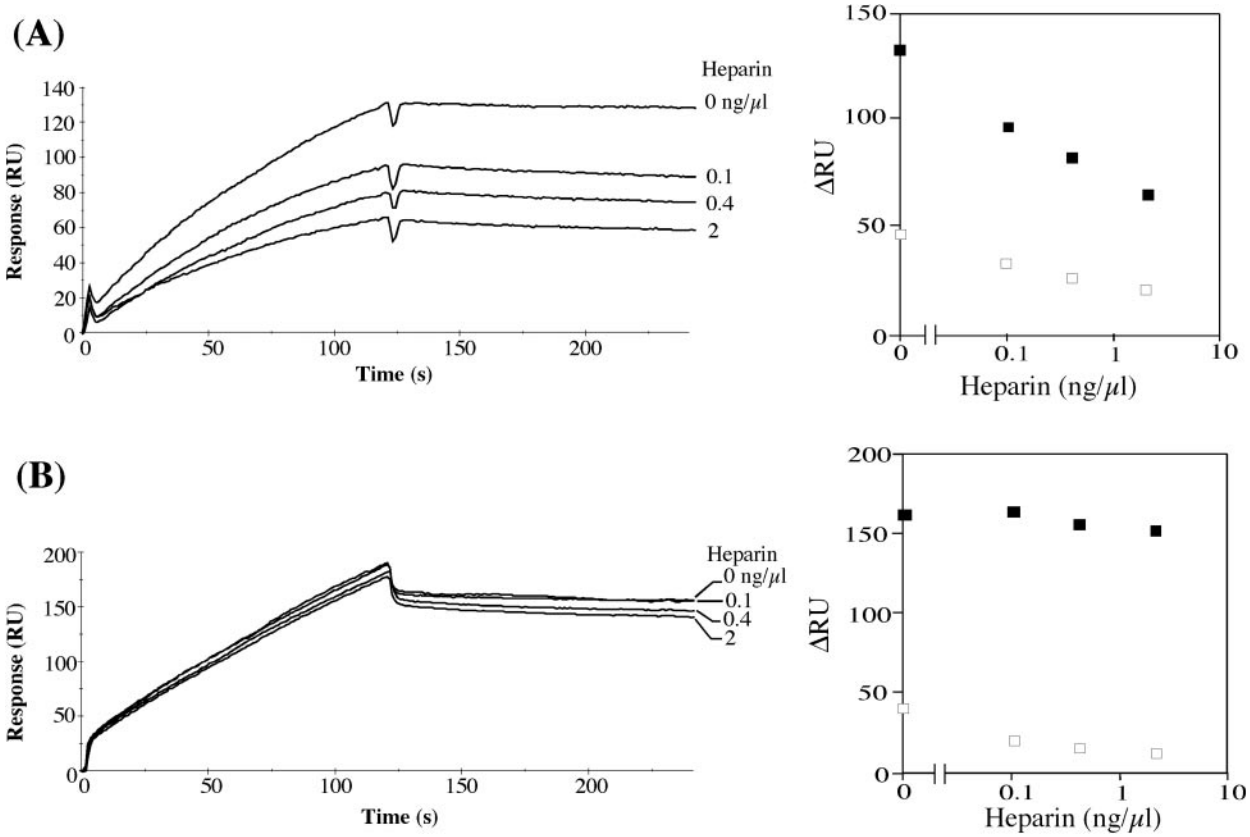

Fig. 5. **The effect of heparin on the interaction between the anti-mPrP aptamer and mPrPs.** (A) Sensorgram of mPrP (10 nM) interaction with immobilized aptamer 60-3 in the presence of heparin (0–2 ng/μl). The observed difference in RU (ΔRU) at each heparin concentration is shown on the right. Closed squares represent interactions with the immobilized aptamer and open squares represent the absence of aptamer. (B) Sensorgram of GST-mPrP$^{89–230}$ (100 nM) interaction with immobilized aptamer 60-3 in the presence of heparin (0–2 ng/μl). The observed ΔRU at each heparin concentration is shown, as in (A). Closed squares represent interactions with the immobilized aptamer and open squares represent the absence of aptamer.

mPrP, suggesting that the deletion of amino-acid residues 23–88 decreases the aptamer-binding affinity to less than 10%. We were unable to detect any binding between aptamer 60-3F and the GST–mPrP$^{155–230}$ deletion variant (data not shown). Furthermore, 60-3F was unable to bind to mPrP$^{120–230}$. These results suggest that the main binding site for aptamer 60-3F is located between amino-acid residues 23 and 119 of mPrP, and that the N-terminus (mPrP$^{23–88}$) is particularly important for strong binding.

As deletion mutants might adopt an alternative conformation to the full-length PrP protein in aptamer recognition, we used the alternative approach of a competitive-binding assay to evaluate the aptamer-binding region. Previous studies have shown that heparin can bind the PrP protein (*24*) at sites located between amino acids 23–52, 53–93 and 110–128 of human PrP (*25*), which correspond to amino acids 23–52, 53–92 and 109–127 of mPrP (Fig. 1). As these binding sites are also in the N-terminal region of PrP, it is important to determine whether heparin interferes with aptamer-mPrP binding. A competitive-binding assay using immobilized aptamer showed that heparin impairs the binding affinity of aptamer 60-3 for mPrP in a dose-dependent manner (Fig. 5A), while GST-mPrP$^{89–230}$ binding is unaffected by heparin (Fig. 5B). Taken together, these results suggest that aptamer 60-3 recognizes and binds to amino-acid residues 23–108 of mPrP.

Secondary Structure Analysis of Aptamer 60-3 by RNase Mapping—To determine the predicted secondary structure of aptamer 60-3 using a Zuker model (*18*), we carried out nuclease mapping with RNase T1 and RNase A. Denaturing 8% PAGE analysis (Fig. 6A) showed that cleavage mainly occurred in single-stranded regions of the predicted secondary structure (Fig. 6B). RNase A cleavage at positions 7 and 20 probably occurs because the stem is UA-rich. Although previous reports have shown that aptamers recognizing PrPs fold into G-quartet structures (*26*, *27*), we did not observe this conformation for aptamer 60-3.

Detection of PrP^{c} in Mouse Brain Homogenate by an RNA Aptamer—We applied aptamers to detect mouse PrP^{C} in a brain homogenate. At first, to check its the binding specificity to PrP^{C}, we precipitated the molecule from normal mouse brain homogenate using 60-3Fb and SA-magnet beads, and found that 60-3Fb binds to the three types of PrP^{C} (non-, mono- and di-glycosylated forms of PrP^{C}; Fig. 7A, Lane 4), the same as antibody (*28*).

Northwestern blotting using a ^{32}P-labeled 60-3F aptamer specifically detected mouse brain PrP^{C} as well as recombinant mPrP (Fig. 7B, Lanes 1 and 2). A 5′-biotinylated aptamer (60-3Fb) used in conventional Western

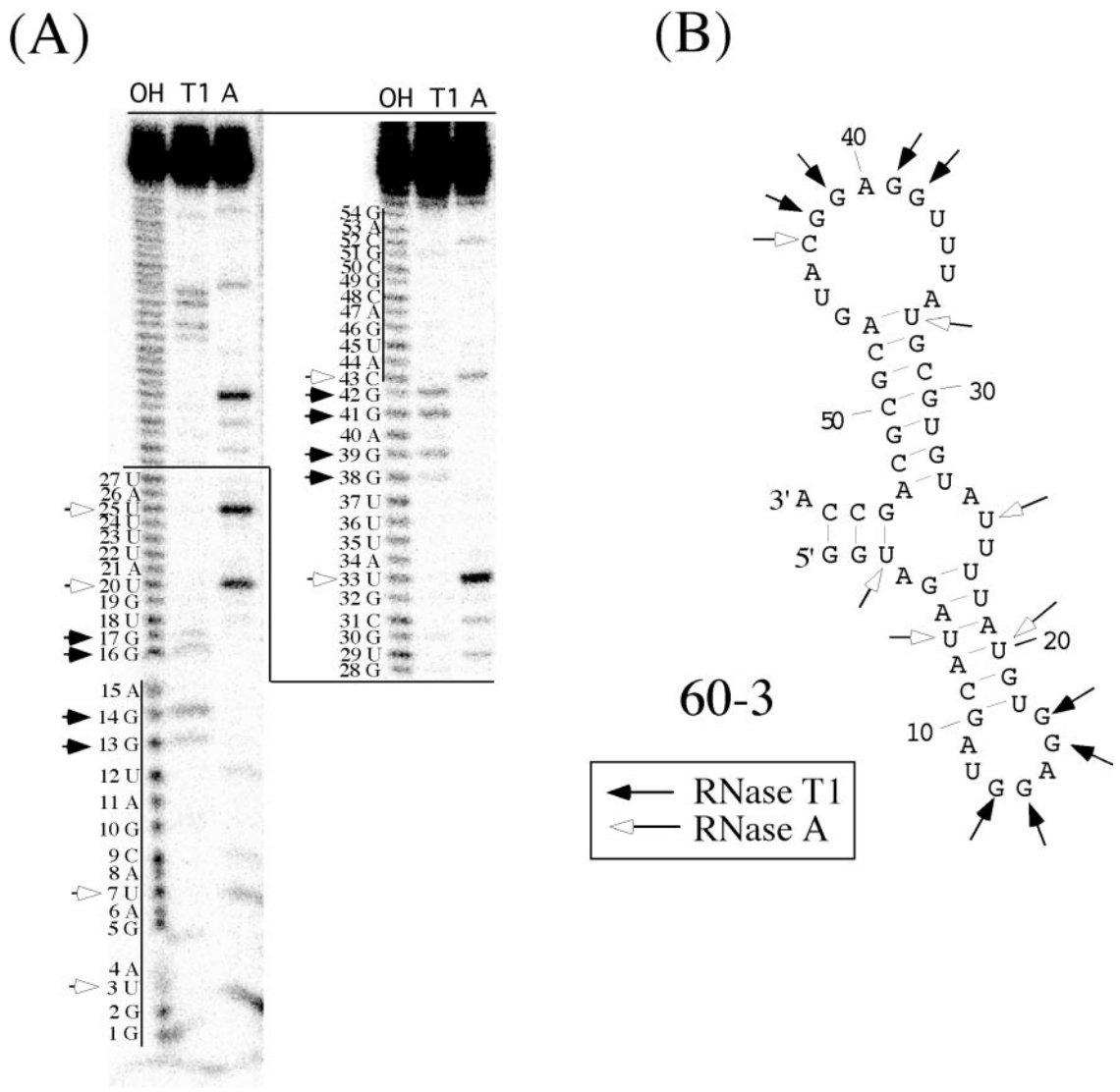

Fig. 6. **Nuclease mapping of anti-mPrP aptamer 60-3.** (A) 5′-^{32}P-labeled aptamer 60-3 was partially digested with RNase T1 (T1) and RNase A (A) and analyzed by 8% PAGE containing 7 M urea. The marker used was an alkaline ladder of aptamer 60-3 (OH). Closed and open arrows represent RNase T1- and RNase A-cleavage sites, respectively. (B) Predicted secondary structure of anti-mPrP aptamer 60-3 using the Zuker model (*18*). Arrows indicate major nuclease cleavage sites.

blotting with SA-AP as a secondary probe also detected mouse PrP^C (Fig. 7B, Lanes 3 and 4) as is detected by the control antibody 6H4 (Lanes 5 and 6). The recognition site of antibody 6H4 is located between amino acids 141 and 150 (*29*).

The protein-concentration detection limit of 60-3Fb for recombinant mPrP was shown by dot-blotting to be approximately 62.5 ng (Fig. 7C). In order to determine whether the aptamer is a viable alternative to antibodies in a conventional blotting assay, we tested the binding affinity of a 5′-biotinylated 2′-methoxy pyrimidine aptamer (60-3OMe). Since 2′-OMe-derivatives are chemically synthesized in large scale, the use of aptamer 60-3 will be easier. Although its affinity for mPrP is slightly weaker than that of the 2′-F modified aptamer (K_d = 47 ± 6 nM; data not shown), we were able to detect mPrP in a similar way.

DISCUSSION

Here we report the isolation of a novel RNA aptamer with a high affinity for mPrP, which can be modified with 2′-F or 2′-OMe pyrimidines for use in nuclease resistance and 5′-biotinylation-detection systems.

Although prion proteins usually bind nucleic-acid molecules in a non-specific manner (*30*, *31*), the RNA aptamers isolated in this study consist of short nucleotide sequences that vary from each other by just a few point mutations. We propose two reasons for this apparent specificity. First, *in vitro* selection was carried out from the sixth round in the presence of a high concentration of competitor RNAs (100–800 μM of tRNA and 10–80 μM of another anti-mPrP RNA aptamer pool). Second, the application of two separation methods, a nitrocellulose filter and magnetic beads, might have concentrated candidates with high-affinity to

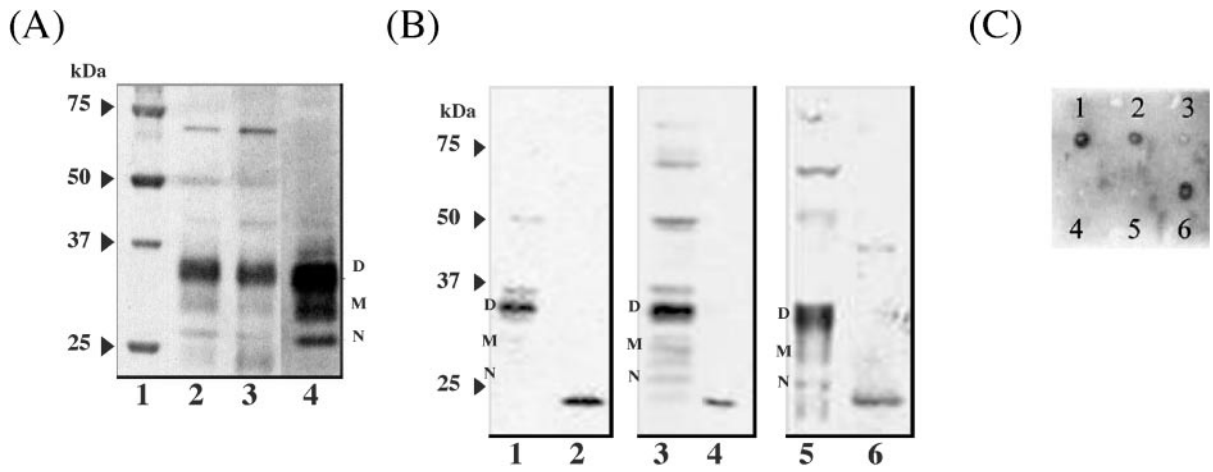

Fig. 7. **Precipitation and detection of PrP in mouse brain homogenate using aptamer 60-3F.** (A) Precipitation of $mPrP^{C}$ using 5′-biotinylated anti-mPrP aptamer (60-3Fb)-coated beads. Molecular weight markers (Lane 1). Mouse brain homogenate (Lane 2). Supernatant (Lane 3) and magnetic beads fraction (Lane 4). N, M and D represent non-, mono- and di-glycosylated forms of mPrP, respectively. PrPs were stained with 6H4 anti-PrP monoclonal antibody and SA-AP conjugate. (B) Lanes 1, 3 and 5 contain 10% ddY mouse brain homogenate, and lanes 2, 4 and 6 contain recombinant mPrP (100 ng). Detection of PrP by 5′-^{32}P-labeled 60-3F. (Lanes 1 and 2). Detection of PrP by 60-3Fb in a Northwestern blotting assay (Lanes 3 and 4). Detection of PrP by 6H4 anti-PrP antibody in an immunoblotting assay (Lanes 5 and 6). (C) Dot-blotting assay of 60-3Fb. Numbers 1–5 represent decreasing concentrations of mounted mPrP (ng) as follows: 1 = 250, 2 = 125, 3 = 62.5, 4 = 31 and 5 = 15.5. Number 6 represents 68 ng mounted SA-AP.

the target molecule. Both aptamer 60-3 and its 2′-F pyrimidine variant 60-3F have high affinities for mPrP (K_d = 5.6 ± 1.5 nM and 22 ± 4 nM, respectively) compared to the previously reported aptamers (*vs.* hamster PrP; K_d = 800 nM, Ref. *26*: *vs.* human PrP; K_d = 1.7 μM, Ref. *27*). This suggests that the 2′OH group of pyrimidines in aptamer 60-3 are not essential for maintaining the tertiary RNA structure required for the interaction with mPrP. The stability and nuclease resistance of the pyrimidine 2′-F–modified aptamer makes it a suitable candidate for bioassay methodologies.

Previous studies have shown that the N-terminal region of PrP has a strong binding affinity for RNA (*26*), and this was confirmed here using deletion variants of mPrP in a filter-binding assay. Moreover, we showed that aptamer 60-3 binds the N-terminal region of mPrP (amino acids 23–88) as well as residues 89–119. From competitive-binding assay studies using heparin, we show that amino-acid residues 23–108 of mPrP bind to aptamer 60-3. This region contains two heparin-binding sites located between residues 23–52 and 53–92; consequently, we demonstrated that heparin impairs mPrP-aptamer 60-3 binding in a dose-dependent manner. In comparison with mPrP, bPrP has an additional octapeptide repeat within the second heparin-binding site 53–92. As this N-terminal region has flexible structure, the lower binding affinity demonstrated by aptamer 60-3 for bPrP compared with mPrP suggests that amino-acid residues 23–52 of mPrP are important for aptamer binding. The tertiary structure of the $mPrP^{23–108}$ region has not been identified using X-ray crystallography or NMR analysis, indicating that this region is an unstructured N-terminus. In this respect, aptamer 60-3 might be of use in future structural analyses of this region.

The aptamer 60-3F was able to detect PrP in a tissue sample, a brain homogenate, similar to a conventional immuno-blotting assay performed with an antibody (Fig. 7B). The aptamer 60-3F showed high affinity for mPrP molecules, which could exclude non-specific binding of various molecules in the homogenate. Furthermore, aptamer 60-3Fb can also be used for bead-based purification and concentration of PrP (Fig. 7A), and for searching for new factor(s) that relate to PrP^{Sc} conformational change.

We thank Dr. Imamura and members of Prion Disease Research Center, National Institute of Animal Health (NIAH) for providing us with the expression plasmids for deletion variants of mPrP and helpful discussions.

REFERENCES

1. Prusiner, S.B. (1982) Novel proteinaceous infectious particles cause scrapie. *Science* **216**, 136–144
2. Pan, K.M., Baldwin, M., Nguyen, J., Gasset, M., Serban, A., Groth, D., Mehlhorn, I., Huang, Z., Fletterick, R.J., and Cohen, F.E. (1993) Conversion of alpha-helices into beta-sheets features in the formation of the scrapie prion proteins. *Proc. Natl. Acad. Sci. USA* **90**, 10962–10966
3. Huang, Z., Gabriel, J.M., Baldwin, M.A., Fletterick, R.J., Prusiner, S.B., and Cohen, F.E. (1994) Proposed three-dimensional structure for the cellular prion protein. *Proc. Natl. Acad. Sci. USA* **91**, 7139–7143
4. Cohen, F.E., Pan, K.M., Huang, Z., Baldwin, M., Fletterick, R.J., and Prusiner, S.B. (1994) Structural clues to prion replication. *Science* **264**, 530–531
5. Scott, M., Foster, D., Mirenda, C., Serban, D., Coufal, F., Walchli, M., Torchia, M., Groth, D., Carlson, G., and DeArmond, S.J. (1989) Transgenic mice expressing hamster prion protein produce species-specific scrapie infectivity and amyloid plaques. *Cell* **59**, 847–857
6. Saborio, G.P., Permanne, B., and Soto, C. (2001) Sensitive detection of pathological prion protein by cyclic amplification of protein misfolding. *Nature* **411**, 810–813

7. Castilla, J., Saa, P., Hetz, C., and Soto, C. (2005) In vitro generation of infectious scrapie prions. *Cell* **121**, 195–206
8. Gajdusek, D.C. (1991) The transmissible amyloidoses: genetical control of spontaneous generation of infectious amyloid proteins by nucleation of configurational change in host precursors: kuru-CJD-GSS-scrapie-BSE. *Eur. J. Epidemiol* **5**, 567–577
9. Prusiner, S.B., McKinley, M.P., Groth, D.F., Bowman, K.A., Mock, N.I., Cochran, S.P., and Masiarz, F.R. (1981) Scrapie agent contains a hydrophobic protein. *Proc. Natl. Acad. Sci. USA* **78**, 6675–6679
10. McKinley, M.P., Bolton, D.C., and Prusiner, S.B. (1983) A protease-resistant protein is a structural component of the scrapie prion. *Cell* **35**, 57–62
11. Bolton, D.C., McKinley, M.P., and Prusiner, S.B. (1982) Identification of a protein that purifies with the scrapie prion. *Science* **218**, 1309–1311
12. Yokoyama, T., Kimura, K.M., Ushiki, Y., Yamada, S., Morooka, A., Nakashiba., T., Sassa, T., and Itohara, S. (2001) In vivo conversion of cellular prion protein to pathogenic isoforms, as monitored by conformation-specific antibodies. *J. Biol. Chem.* **276**, 11265–11271
13. Ellington, A.D. and Szostak, J.W. (1990) In vitro selection of RNA molecules that bind specific ligands. *Nature* **346**, 818–822
14. Tuerk, C. and Gold, L. (1990) Systematic evolution of ligands by exponential enrichment: RNA ligands to bacteriophage T4 DNA polymerase. *Science* **249**, 505–510
15. Tombelli, S., Minunni, M., and Mascini, M. (2005) Analytical applications of aptamers. *Biosensors & Bioelectronics* **20**, 2424–2434
16. Jenison, R.D., Gill, S.C., Pardi, A., and Polisky, B. (1994) High-resolution molecular discrimination by RNA. *Science* **263**, 1425–1429
17. Kikuchi, K., Umehara, T., Fukuda, K., Hwang, J., Kuno, A., Hasegawa, T., and Nishikawa, S. (2003) RNA aptamers targeted to domain II of hepatitis C virus IRES that bind to its apical loop region. *J. Biochem.* **133**, 263–270
18. Zuker, M. (1989) Computer prediction of RNA structure. *Methods Enzymol.* **183**, 202–287
19. Fukuda, K., Vishnuvardhan, D., Sekiya, S., Hwang., J., Kakiuchi, N., Taira, K., Shimotohno, K., Kumar, P.K.R., and Nishikawa, S. (2000) Isolation and characterization of RNA aptamers specific for the hepatitis C virus nonstructural protein 3 protease. *Eur. J. Biochem.* **267**, 3685–3694
20. Hwang, J., Fauzi, H., Fukuda, K., Sekiya, S., Kakiuchi, N., Shimotohno, K., Taira, K., Kusakabe, I., and Nishikawa, S. (2000) The RNA aptamer-binding site of hepatitis C virus NS3 protease. *Biochem. Biophys. Res. Commun.* **279**, 557–562
21. Bagga, P.S. and Wilusz, J. (1999) Northwestern screening of expression libraries. *Methods Mol. Biol.* **118**, 245–256
22. Cummins, L.L., Owens, S.R., Risen, L.M., Lesnik, E.A., Freier, S.M., McGee, D., Guinosso, C.J., and Cook, P.D. (1995) Characterization of fully 2′-modified oligonucleotide hetero- and homoduplex hybridization and nuclease sensitivity. *Nucleic Acids Res* **23**, 2019–2024
23. Ruckman, J., Green, L.S., Beeson, J., Waugh, S., Gillette, W.L., Henninger, D.D., Claesson-Welsh, L., and Janjic, N. (1998) 2'-Fluoroprymidine RNA-based aptamers to the 165-amino acid form of vascular endothelial growth factor ($VEGF_{165}$). *J. Biol. Chem.* **273**, 20556–20567
24. Caughey, B., Brown, K., Raymond, G.J., Katzenstein, G.E., and Thresher, W. (1994) Binding of the protease-sensitive form of PrP (prion protein) to sulfated glycosaminoglycan and congo red. *J. Virol.* **68**, 2135–2141
25. Warner, R.G., Hundt, C., Weiss, S., and Turnbull, J.E. (2002) Identification of the heparan sulfate binding sites in the cellular prion protein. *J. Biol. Chem.* **277**, 18421–18430
26. Weiss, S., Proske, D., Neumann, M., Groschup, M.H., Kretzschmar, H.A., Famulok, M., and Winnacker, E.L. (1997) RNA aptamers specifically interact with the prion protein PrP. *J. Virol.* **71**, 8790–8797
27. Proske, D., Gilch, S., Wopfner, F., Schatzl, H.M., Winnacker, E.L., and Famulok, M. (2002) Prion-protein-specific aptamer reduces PrPSc formation. *Chembiochemistry* **3**, 717–725
28. Hay, B., Barry, R.A., Lieberburg, I., Prusiner, S.B., and Lingappa, V.R. (1987) Biogenesis and transmembrane orientation of the cellular isoform of the scrapie prion protein. *Mol. Cell Biol.* **2**, 914–920
29. Korth, C., Stierli, B., Streit, P., Moser, M., Schaller, O., Fischer, R., Schulz-Schaeffer, W., Kretzschmar, H., Raeber, A., Braun, U., Ehrensperger, F., Hornemann, S., Glockshuber, R., Riek, R., Billeter, M., Wuthrich, K., and Oesch, B. (1997) Prion (PrP^{Sc})-specific epitope defined by a monoclonal antibody. *Nature* **390**, 74–77
30. Nandi, P.K. (1997) Interaction of prion peptide HuPrP106–126 with nucleic acid. *Arch. Virol.* **142**, 2537–2545
31. Nandi, P.K. and Nicole, J.C. (2004) Nucleic acid and prion protein interaction produces spherical amyloids which can function in vivo as coats of spongiform encephalopathy agent. *J. Mol. Biol.* **344**, 827–837